Proceedings of the ASME 2013 32nd International Conference on Ocean, Offshore and Arctic Engineering
OMAE2013
June 9-14, 2013, Nantes, France

OMAE2013-11446

NUMERICAL MODELING OF WAKE EFFECT ON AQUACULTURE NETS

Per Christian Endresen
SINTEF Fisheries and Aquaculture
Trondheim, Norway
per.christian.endresen@sintef.no

Martin Føre
SINTEF Fisheries and Aquaculture
Trondheim, Norway
martin.fore@sintef.no

Arne Fredheim
SINTEF Fisheries and Aquaculture
Trondheim, Norway
arne.fredheim@sintef.no

David Kristiansen
SINTEF Fisheries and Aquaculture
Trondheim, Norway
david.kristiansen@sintef.no

Birger Enerhaug
SINTEF Fisheries and Aquaculture
Trondheim, Norway
birger.enerhaug@sintef.no

ABSTRACT

Accurate modeling of drag forces on net cages due to water current is important when designing floating fish farm systems. These drag forces give a major contribution to the total environmental forces on a fish farm, especially mooring line forces. When subjected to current, the net cage will deform. High current velocities can result in large deformations and lead to collapse of the net cage. For circular fish farms with a flexible floating collar, large deformations may induce contact between the weighting system and the net, resulting in abrasion that can cause tearing of the net material and consequently failure that will lead to fish escape.

The motivation for this paper is to obtain a better understanding and more accurate model for drag forces and corresponding deformations of circular net cages due to water current. Calculation of drag forces on a net cage is complicated due to the porous nature of the net, geometry and flexibility of the system. Adding to the complexity is the wake effect, or reduced velocity, behind each individual twine which will have a significant effect on the forces and deformations of the net cage. This wake effect will result in reduced inflow velocity on parts of the net being downstream.

A method for estimating wake effects acting within an aquaculture net structure was developed and implemented in a numerical code taking net deformation into account. Numerical simulations of a cylindrical net cage were compared with experimental results. Comparison between simulations with and without wake effect revealed a reduction in total drag up to 22% when wake effect was applied. Although the model consistently overestimated drag forces on the net cage (average deviation of 25%), simulation results compared well with measurement data, particularly for low current velocities where deviations were as low as 7%. This indicates a consistent wake effect and drag model that produces conservative estimates of drag forces on net cages.

1. INTRODUCTION

An object immersed in uniform water current will have both upstream and downstream effects on the velocities [2]. For slender geometries, like twines used in aquaculture nets, the dominant effect will be downstream. In a net structure placed in uniform water current, segments of the net that are downstream from other net segments will therefore experience a lower incident water velocity than upstream net segments. In order to accurately calculate the drag forces on aquaculture nets due to water current, this reduction in water velocity, or wake effect, needs to be properly accounted for. For earlier (and important) work on this subject, see [7, 8].

In this study a method for calculation of wake effect on flexible aquaculture nets with quadratic meshes, based on Blevins virtual origin for circular cylinders [1, 2], was derived. The method was implemented in SINTEF Fisheries and Aquaculture's in-house software FhSim, in which wake effects are included in calculations of drag forces on net structures. Comparisons of drag forces between numerical simulations and experimental data for a flexible cylindrical net cage in uniform

water current were carried out to evaluate how accurately the wake model estimated velocity reduction caused by twines in the netting.

NOMENCLATURE

U_∞	Incident (undisturbed) current velocity
u	Velocity reduction experienced at coordinates (x,y) in a 2D plane
U_i	Current velocity at cylinder i of $N+1$ consecutive cylinders
U_{eqv}	Equivalent or average velocity for all twines in a net panel due to local wake effects
u_{Dv}, u_{Dh}	Velocity reduction caused by vertical and horizontal bars in upstream panel
U_{DS}	Incident velocity to a panel downstream from other net segments
U_{GL}	Input velocity to force calculations in numerical code, adjusted due to local and global wake effects
C_d	Reynolds number dependent drag coefficient for a circular cylinder
F_x	Drag force
Rn	Reynolds number
Sn	Ratio of projected area of netting material and net panel area (solidity)
x_i, y_i	Coordinates of vertical twine i in a panel
x_j, z_j	Coordinates of horizontal twine j in a panel
x_{DS}, y_{DS}, z_{DS}	Coordinates of centroid in a net panel downstream from other net segments
x_{US}, y_{US}, z_{US}	Coordinates of centroid in a net panel upstream from other net segments
d	Cylinder diameter used in derivation of wake effect formulas
d_t	Twine diameter
l_b	Bar length (distance between the centers of two knots)
α	Angle of attack (angle between panel and flow direction)
D_{US}	Distance between a downstream panel and a upstream panel
K_G	Reduction factor due to global wake effects used in numerical code
K_L	Reduction factor due to local wake effects used in numerical code

2. MATERIALS AND METHODS

Numerical model framework

Simulations of aquaculture nets in FhSim are performed using an element based approach where triangular net elements interconnected by a set of nodes [10, 11, 12] are used to model arbitrary net structures. Hydrodynamic and gravitational loads acting on the net are calculated separately for each element and then distributed onto the three nodes associated with the element. Further, external forces acting on the net structure (e.g. from ropes, floating collars and weights) affect the net through the nodes, thus the distribution of forces through a simulated net structure is realized through the nodes interconnecting the elements.

Complex net structures, such as net cages, would have to be built up of a large number of net elements in FhSim in order to obtain sufficient flexibility to replicate realistic deformations when subjected to hydrodynamic forces. Each of these net elements would then typically represent several similarly oriented meshes in the simulated net, and the hydrodynamic forces acting on the element would then be found by computing a Morison-type cross flow drag and lift for a single twine (in each of the two twine orientations within the element) and one knot, and then multiplying the results by the number of twines and knots comprising the element, respectively. Consequently, the inclusion of wake effects into this model would have to be realized at two abstraction levels; the wake effects acting between the mesh bars comprising an element and the wake effects acting between separate net elements. It was thus necessary to derive expressions for both element-internal (local) wake effects and inter-elemental (global) wake effects.

For further details on the structural and hydrodynamic load model used to simulate net structures in FhSim, see [3].

Local wake effect

For full scale aquaculture nets subjected to current the Reynolds number will generally be large enough to assume turbulent wake behind the twines. The wake, according to [13], becomes turbulent for $Rn > 300$. Thus, a model for turbulent wake can be used to estimate reduction in velocity behind twines in the net.

For uniform flow around a 2D circular cylinder in infinite fluid, Blevins virtual origin formula [1, 2] for turbulent wake can be used to estimate the velocity reduction downstream from the cylinder. The normalized velocity deficit downstream from a 2D circular cylinder placed at the origin (x=0, y=0) is given as:

$$(1)\quad \frac{u}{U_\infty} = 1.2\sqrt{\frac{C_d}{6+\frac{x}{d}}}\,exp\left\{\frac{-\left(\frac{y}{d}\right)^2}{0.0767C_d\left(6+\frac{x}{d}\right)}\right\}$$

where u and U_∞ are the velocity reduction experienced at the coordinate (x,y) and the undisturbed water velocity, respectively. The positive x-axis is oriented along the incident velocity vector, C_d is the Reynolds number dependent drag coefficient for a circular cylinder and d is the cylinder diameter.

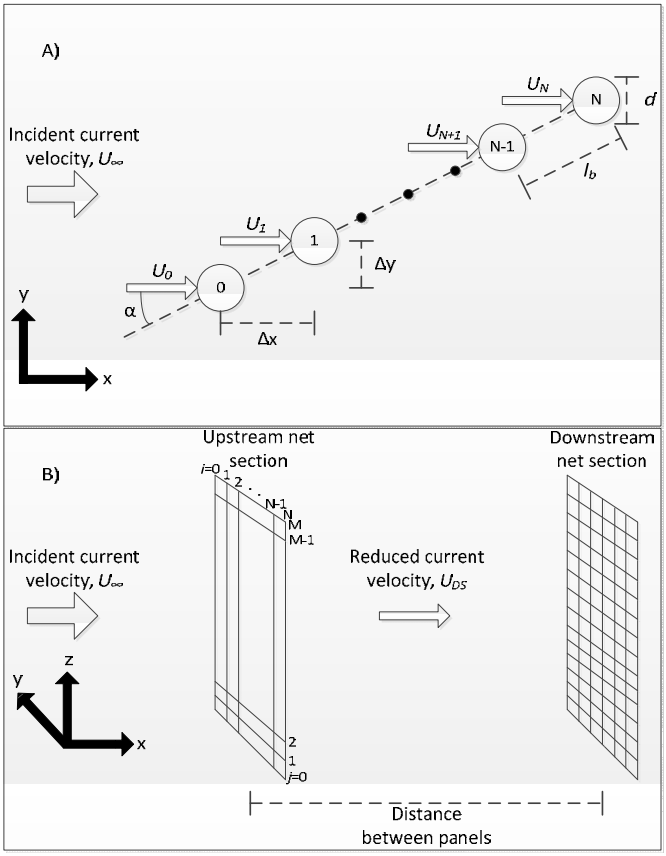

Figure 1: A) Illustration of the local wake effect concept, where a grid of N+1 cylinders (cross section of a net panel) with diameter *d* are exposed to an incident current velocity U_∞. U_i (*i* = 0, 1, … , N-1, N) denotes the velocity experienced by cylinder *i*, which is modified due to the presence of preceding cylinders. B) Illustration of global wake effect where the upstream (left) net section is exposed to an incident current velocity U_∞. Wake effects from the upstream net section results in a reduced incident current velocity (U_{DS}) at the downstream net section.

The first step in finding the velocity reduction on individual twines in a net panel is to find a simplified description of the panel in a 2D (*xy*) plane (Figure 1 A). As for equation (1), the positive x-axis of the 2D plane is oriented along the incident current velocity vector. A staggered grid of cylinders with constant distance Δ*x* and Δ*y* between the cylinders is then used to represent a cross section of a panel were one of the two net twine axes directions is perpendicular to the incident velocity while the other twine axis is in the xy-plane (henceforth denoted ideal panel orientation). Δ*x* and Δ*y* are defined by the angle of attack (α) between the cylinder grid and the incident current velocity (U_∞) and the mesh bar length (l_b). Within the panel, contributions to velocity reduction from twines in the xy-plane are thought to be small compared to twines with axis perpendicular to the incident current. Contribution to local wake effect from twines in the xy-plane is therefore neglected. Since equation (1) is linear with respect to *u*, contributions from individual twines can be added to obtain the velocity reduction on a given cylinder caused by preceding cylinders. For *N+1* cylinders the normalized velocity on cylinder *N*, according to [4], can be expressed as the sum of velocity deficits from preceding cylinders subtracted from the incident current velocity.

$$(2)\quad \frac{U_N}{U_\infty} = 1 - \sum_{i=0}^{N-1} \frac{U_i}{U_\infty} 1.2 \sqrt{\frac{C_d}{6+\frac{x_N - x_i}{d}}} exp\left\{ \frac{-\left(\frac{y_N - y_i}{d}\right)^2}{0.0767 C_d \left(\frac{x_N - x_i}{d}\right)} \right\}$$

U_N and U_i are the velocity at the center of cylinder *N* and cylinder *i*, respectively. x_N and x_i are the *x*-positions of cylinder *N* and *i*. y_N and y_i are the *y*-positions. The effects of all preceding cylinders are included, thus the velocity at the center of each cylinder needs to be calculated starting with the cylinder farthest upstream followed by the succeeding cylinders. In [4], a constant of 1.02 is used in equation (2) to account for mass conservation through the cylinder grid. However, since mass conservation in the FhSim framework is handled by local increase in velocity through the meshes (see [3]), the original parameter of 1.2 from [2] is used. According to [2], equation (2) is valid in the fully developed region of the wake, which occur 20 to 50 diameters downstream from the cylinder. In [4], good general agreement, when comparing numerical results with experiments, was obtained for five cylinders in a row and staggered arrangement with a length between cylinders of five diameters. This is applicable to aquaculture nets, and equation (2) is thus used. Also, experiments with two cylinders in tandem [14], show steady drag forces for a ratio between length between cylinders and cylinder diameter larger than 7. In these experiments, *Rn* = 3400.

Normalized drag force on a cylinder grid can be calculated by adding the contributions from all cylinders.

$$(3)\quad \frac{F_x}{\rho d U_\infty^2} = \frac{C_d}{2U_\infty^2}\left(U_0^2 + U_1^2 + \cdots + U_N^2\right)$$

Dimension for F_x is *N/m*. In order to calculate drag forces by use of the element based method in FhSim, an equivalent average velocity for all twines in a panel must be found. For the cylinder grid presented previously, normalized drag force can be expressed as $F_x/\rho d U_\infty^2 = (C_d/2U_\infty^2)(N+1)U_{eqv}^2$. Setting this expression equal to equation (3) yields

$$(4)\quad \frac{U_{eqv}}{U_\infty} = \sqrt{\frac{1}{N+1}\sum_{i=0}^{N}\left(\frac{U_i}{U_\infty}\right)^2}$$

where U_{eqv} is the equivalent or average velocity on the cylinders.

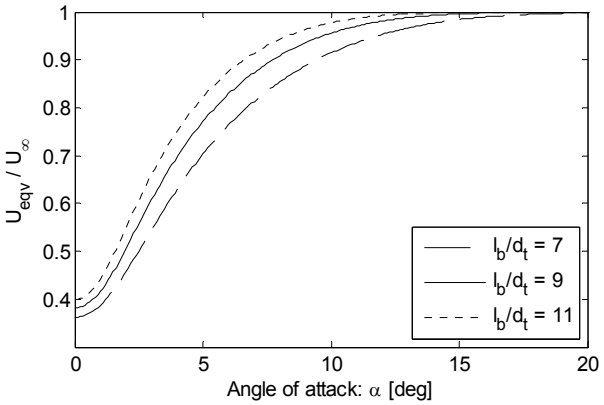

Figure 2: U_{eqv}/U_∞ for a staggered cylinder grid (20 cylinders) as a function of angle of attack (α) for three different l_b/d_t relationships. The drag coefficient (C_d) is set to 1.1. Values are plotted for the range of α for which local wake effects are most notable (0 to 20°).

Since the result from equation (4) depends on Δx and Δy, U_{eqv} is dependent on α as well as l_b and d_t. For most net types relevant for aquaculture, l_b and d_t are such that U_{eqv} will only be notably different from U_∞ for α between 0 and 20° (Figure 2). However, since U_{eqv} is highly dependent on both the angle of attack (α) and the ratio between bar length and twine diameter (l_b/d_t), local wake effect can be experienced for α > 20° for low ratios of l_b/d_t. Local wake effect is therefore, in order to have a more generic method, evaluated for α = 0° to α = 30°.

Global wake effect

Approximately 50% of the net comprising a cylindrical net cage will experience reduced current velocities due to wake caused by parts of the net placed upstream. For a net cage with horizontal center in x = 0 in uniform water current along the positive x-axis, all panels with a center position x < 0 will affect one or more panels downstream (for a non-deformed geometry).

Unlike for the simplified 2D approach used to find local wake effects, the computation of the global wake effect caused by a panel needs to take both net twine axes directions into account. Effects from vertical bars (perpendicular to the xy-plane, see Figure 1 A) and horizontal bars (in the xy-plane) were therefore computed separately and then summed to produce a total value for the global wake effect caused by an upstream panel on downstream panels (Figure 1 B).

The contribution to the global wake effect caused by vertical bars (u_{Dv}/U_∞) was found by first computing the normalized current velocities (U_i) at all N vertical bars in the upstream panel using equation (2). The impact of these bars on the global wake effect was then found as:

$$(5)\quad \frac{u_{Dv}}{U_\infty} = \sum_{i=0}^{N-1} \frac{U_i}{U_\infty} 1.2 \sqrt{\frac{C_d}{6+\frac{x_{DS}-x_i}{d}}} exp\left\{\frac{-\left(\frac{y_{DS}-y_i}{d}\right)^2}{0.0767 C_d\left(\frac{x_{DS}-x_i}{d}\right)}\right\}$$

where x_{DS} and y_{DS} are the xy-coordinates for the centroid of the downstream panel. u_{Dv} is the velocity reduction due to vertical bars.

A similar exercise was performed to find the contribution from the horizontal bars in the panel (u_{Dh}/U_∞) by employing the xz-plane rather than the xy-plane as horizontal bars are perpendicular to the z-axis. All horizontal bars in an ideal panel will be inclined towards the current (Figure 1). As explained previously, these bars will not contribute significantly to the local wake effect, but they will themselves be subjected to the local reduced velocity and cause a global wake effect. Since no point on an inclined bar will be the same distance from the downstream panel or experience the same locally reduced velocity, the average velocity U_{eqv} from equation (4) and the centroid to centroid distance between the upstream and downstream panel are used instead of the velocity on each bar in the upstream panel (U_i) and the horizontal distance between individual bars in the upstream panel and the centroid of the downstream panel. Hence, the following expression was used to estimate the velocity reduction u_{Dh}/U_∞:

$$(6)\quad \frac{u_{Dh}}{U_\infty} = \sum_{j=0}^{M-1} \frac{U_{eqv}}{U_\infty} 1.2 \sqrt{\frac{C_d}{6+\frac{x_{DS}-x_{US}}{d}}} exp\left\{\frac{-\left(\frac{z_{DS}-z_j}{d}\right)^2}{0.0767 C_d\left(\frac{x_{DS}-x_{US}}{d}\right)}\right\}$$

where z_j represents the z-position of bar j (horizontal), and x_{US} is the x-coordinate of the centroid of the upstream panel. u_{Dv} and u_{Dh} were then subtracted from U_∞ to yield the total global wake effect caused by an upstream panel on downstream panels:

$$(7)\quad \frac{U_{DS}}{U_\infty} = 1 - \frac{u_{Dv}+u_{Dh}}{U_\infty}$$

Consequently, U_{DS} represents the incident current velocity to a downstream panel (Figure 1 B). For α = 90° on the upstream panel the presented method is comparable with the sum of cylinders method in [7, 8].

As seen from equation (5) and (6) transverse variation of reduced velocity over the downstream panel is neglected. This is an error source in the calculation, but can be justified since neighbors to the upstream panel also can affect the downstream panel, which is not included here. Therefore, the largest velocity deficit, which occurs in a straight line in the incident current direction behind the upstream panel, is used. Effects from neighbors to the upstream panel will smooth out the transverse velocity variation downstream, i.e. create an even reduction over the panel, but not increase or decrease the maximum value significantly. This is also in accordance with [7, 8] where it is found that transverse velocity variation behind a net panel is small, except at the boundaries of the wake. Since a commercial net cage consist of a continuous net, except at the surface, such high transverse variations in the wake field as described for a single net panel is not likely to exist inside a net cage. Hence, the maximum velocity reduction from one

upstream panel on a downstream panel is a good approximation of the average velocity reduction experience by a downstream panel due to wake effect from several upstream panels.

Implementation of local wake effect in FhSim

Since FhSim is based on numerical integration, it is undesirable to evaluate equation (2) to (4) for each time step to find the equivalent velocity of the twines in a net element, as this could greatly increase the computational load of the elements. Consequently, a polynomial estimate of the equivalent velocity for each net element as a function of angle of attack (α) was derived and used during simulation.

The derivation of the polynomial was performed during model initialization, where the expression in equation (2) was evaluated over all N twines in the element for α between 0° and 30°. This operation produced a set of values describing U_{eqv}/U_∞ as a function of α between 0 and 30° (similar to the curves in Figure 2). A seventh order polynomial estimating the resulting curve for U_{eqv}/U_∞ as a function of α was then found by least-squares fitting for each element. This polynomial was used to estimate the value of U_{eqv}/U_∞ during simulation, with the present α as an input parameter. α is the angle of attack between the incident current velocity vector and the plane of the triangular net element. A polynomial is not presented here since it will be dependent on both the ratio l_b/d_t and the number of bars (N and M) comprising each panel in the numerical setup.

Implementation of global wake effect in FhSim

To include global wake effects in the model, net elements that are located downstream from other sections of the net have to be identified. A straight-forward solution to this problem could be to let each net element evaluate their position relative to all other elements in the model, and thus determine whether they are affected by global wake effects. This would however, introduce excessive numerical loads during simulation. A less generic but more numerically efficient method was therefore developed.

The method was based on the assumptions that the cage is cylindrical and that the current direction does not change during simulation. By using the initial geometry of the cage along with the current direction vector, a plane intersecting the cage through the center was identified. This plane was perpendicular to the incident current vector, thus all elements located downstream from the plane would be affected by global wake effects caused by the elements located upstream from the plane (Figure 3).

During simulation initialization, the net elements downstream from the intersecting plane were identified as being subject to global wake effects. These elements were also provided with a nominal distance to the upstream panel (D_{US}) which was calculated as 2 times the distance between the initial position of their centroid and the intersecting plane. The incident velocity to a downstream panel (U_{DS}) was assumed to be affected by the global wake effect of a net segment with the same size and orientation as itself. Consequently, U_{DS}/U_∞ for a downstream panel in the model was calculated by evaluating equation (5) to (7) using the orientation and size of the panel itself, but by exchanging the expression $x_{DS} - x_{US}$ with D_{US}. A downstream panel will in reality (for a non-deformed geometry) be equal to an upstream panel mirrored around the intersecting plane (yz-plane) shown in Figure 3. Since reduced incident velocity on a downstream panel is calculated in the centroid of the panel, the above described procedure for calculation of global wake effect can be used.

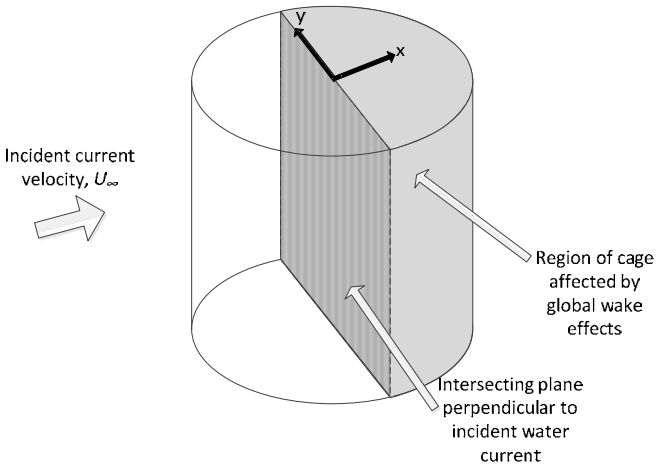

Figure 3: Illustration of method to identify the parts of a cylindrical net cage which will experience global wake effects caused by upstream net segments.

This operation was performed for angles of attack (α) between 0 and 90°, yielding a set of values for U_{DS}/U_∞ pertaining to the full range of angles of attack. As with the local wake effect, the resulting set of values was approximated by a seventh order polynomial in α.

Impact on force calculations in FhSim

During simulation of net structures in FhSim, each net element uses the water velocity at their centroid to compute hydrodynamic forces. To include the wake effect into these computations, each element first evaluated their polynomial for global wake effect based on their angle of attack (α), yielding a reduction factor K_G which represented an estimate of the reduction caused by the wake of upstream net sections. For elements that were not downstream from other parts of the net, K_G was set to 1, meaning no reduction due to global wake effects. K_G was then multiplied with the incident water current velocity (U_∞) resulting in an incident current velocity corrected for global wake effects (U_G). Subsequently, the elements evaluated their local wake polynomials as a function of α, producing a reduction factor K_L representing an estimate of the internal wake effects within the panel. When α >30°, this factor was set to 1. K_L was then multiplied with U_G, returning the incident current velocity corrected for both global and local

wake effects (U_{GL}). U_{GL} was then used as the input to the functions used to compute hydrodynamic forces on the net element.

3. RESULTS

Single panel simulations

To verify the functionality of the local wake effect, a series of simulations of a 1 x 1 m net panel were performed. The panel (and the mesh bars) was ideally oriented relative to the incident water current. To prohibit deformation, the corners of the net panel were fixed in space, while the incident water current was set at 0.5 ms^{-1}, encountering the panel at angles of attack between 0° and 30°. The twine diameter was set to 1.8 mm while the mesh bar length was set to 16 mm. Simulations were performed both with and without the local wake effect to investigate the impact of local wake effects on drag forces in the model (Figure 4). The forces acting on the panel with no local wake effect were clearly higher than those acting on the panel with local wake effect for $\alpha < 15°$ (Figure 4). For higher angles of attack, the forces on the two panels were comparable.

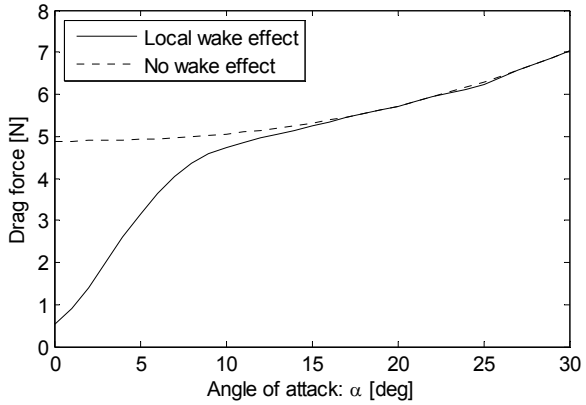

Figure 4: Drag force for simulations in FhSim with and without wake effect for 1 x 1 m panel subjected to a current velocity of 0.5 ms^{-1}.

Global wake effect

In order to evaluate the global wake model, the calculated reduced velocity downstream from a net panel is compared with results from [7, 8] (Figure 5). Experimental results in [7] for a net panel with attack angle of 90° and solidity (Sn) of approximately 0.24 revealed a reduction factor of approximately 0.84, while the calculation model in [7] predicted a reduction factor equal to 0.85. A reduction factor of 0.85 means that the water velocity downstream from the panel is reduced to 85% of the undisturbed incident current velocity to the panel. Our method produced similar results, giving a reduction factor of 0.84 for Sn = 0.225 and 0.83 for Sn = 0.24. Solidity is calculated as $Sn = 2d_t/l_b$. A panel with Sn = 0.24 from [7] was chosen since this was the net with a solidity value most comparable to the one used in [6].

Figure 6 illustrates how the velocity reduction behind a panel computed with our method varies with angle of attack. Velocities were evaluated for three solidities at a distance equal to 800 twine diameters. This is equal to the diameter of the net cage used in [6]. From the figure it can be seen, as expected, that reduction in water velocity increases as the solidity increases. In contradiction to local wake effect (Figure 4), velocity behind the panel is greatly reduced for angles of attack up to approximately 30°. Numerical results from a 100 x 100 twine net panel where chosen since a further increase in number of twines not affected the magnitude of the velocity reduction for angles of attack above 2.5°. For the numerical results in Figure 5 and Figure 6 the drag coefficient C_d (in equation (2), (3), (5) and (6)) was set to a fixed value of 1.2. When calculating wake effects and drag forces on net structures in FhSim, the drag coefficient is Reynolds number dependent [3].

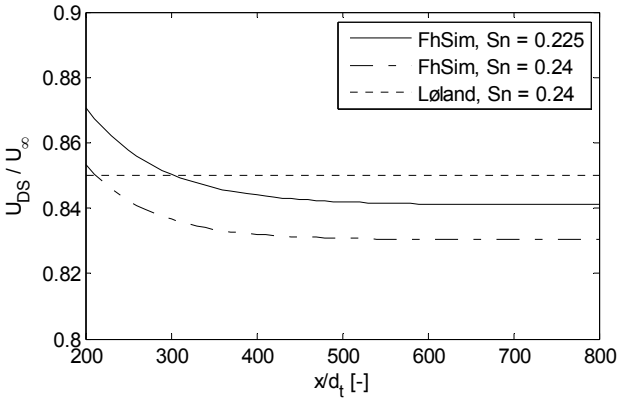

Figure 5: Comparison of velocity reduction downstream from a net panel with an angle of attack of 90°. The panel consists of 100 x 100 twines. x is the distance behind the panel in the incident current direction.

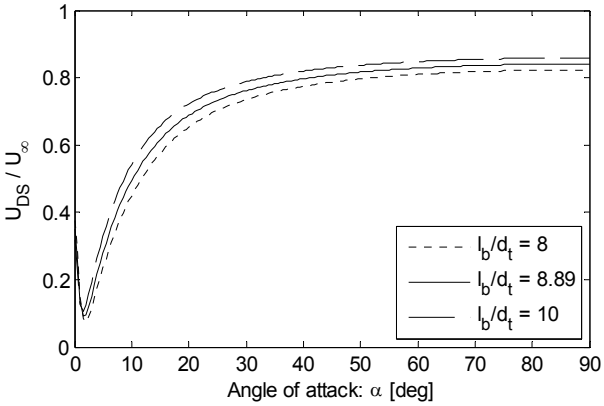

Figure 6: Velocity reduction (ratio between water velocity behind the panel and undisturbed current velocity) downstream from a 100 x 100 twine net panel as a function of the panels attack angle. Numerical results for three solidities of approximately 0.25 (l_b/d_t=8), 0.225 (l_b/d_t=8.89) and 0.2 (l_b/d_t=10) are shown. Reduced velocity is evaluated 800 twine diameters downstream.

Comparison with measurement data for a cylindrical net cage

To validate both local and global wake effects a series of simulations based on a set of published experiments conducted in a flume tank [6] were performed. In this study, the authors used a cylindrical net structure with a twine diameter of 1.8 mm and a bar length of 16 mm, which equates to a net solidity of approximately 0.225. The top of the net structure was attached to a rigid circular hoop that was placed horizontally about 1 m beneath the water surface. 16 weights were attached to the net bottom. The net spanned a diameter of 1.435 m, while its depth was 1.44 m. To gauge the forces acting on the net, the hoop was attached to four load cells which also served to fix the top position and orientation of the net. The net was subjected to six different water current velocities ranging from 0.04 to 0.52 ms^{-1}, and bottom weights of 400, 600 and 800 g (henceforth referred to as weight case 1 (WC1), WC2 and WC3).

To produce data comparable to those presented by [6], a total of 14 simulation scenarios were set up (WC1, WC2: 5 velocities 0.13 - 0.52 ms^{-1}, WC3: 4 velocities 0.21 - 0.52 ms^{-1}). This corresponds to a minimum and maximum Reynolds number of 234 and 936, respectively. The net structure was modeled using 128 net panels with similar twine diameters and bar lengths as in the experiments. The net panels were organized in a cylindrical shape, the top side nodes of which were fixed in space. Sixteen of the bottom nodes of the simulated structure were subjected to external vertical forces equivalent to the weight in water of the weights used in the experiments. Simulations were performed for all 14 cases, and the total forces acting on the simulated structure were obtained by summing up the forces acting on the top side nodes. All simulations were performed both with and without wake effects activated to evaluate the effect of wake effects on the models ability to estimate the drag forces observed in the experiments by [6].

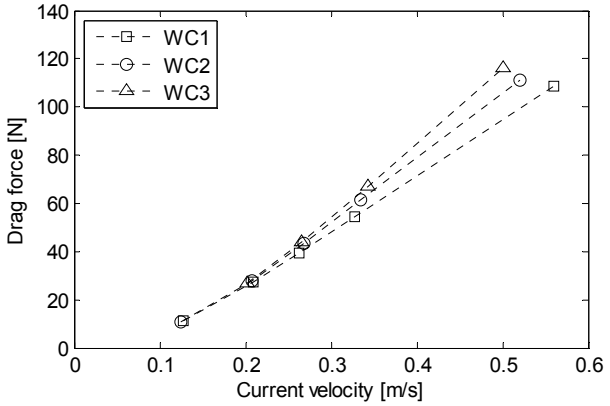

Figure 7: Drag forces for simulations of weight case 1 (WC1), WC2 and WC3. Wake effect is included.

Figure 7 shows results from simulations of the three different bottom weight configurations. Drag forces were similar for the three weight cases up to a current velocity of 0.21 ms^{-1}, while there were some differences for velocities ranging from 0.21 ms^{-1} to 0.33 ms^{-1} (Figure 7). For higher velocities, drag depended more on the weights, with increased drag with increasing bottom weight. These results compare well to [6], where the authors experienced no drag weight dependency up to a velocity of 0.21 ms^{-1}, a small dependency from 0.21 ms^{-1} to 0.33 ms^{-1} and a clear connection between drag and weight for larger velocities.

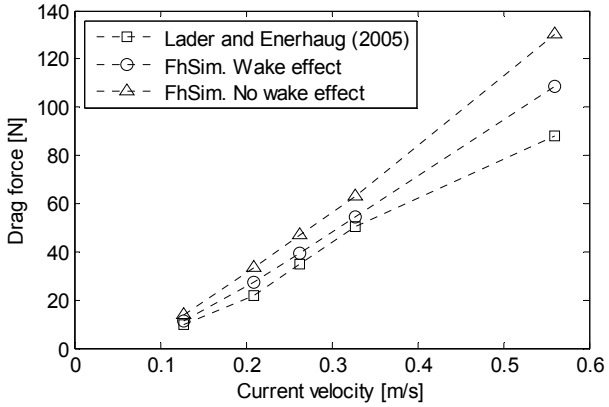

Figure 8: Comparison of drag forces for WC1. Results from simulations with and without wake effect and experiments from [6] are shown.

For WC1, the model output with wake effects compared well with the observed data for the lowest four velocities, overestimating the drag forces with 15% on average, the lowest deviation occurring at 0.33 ms^{-1} with 7% (Figure 8). Deviations were somewhat larger for 0.52 ms^{-1} with 23% overestimation.

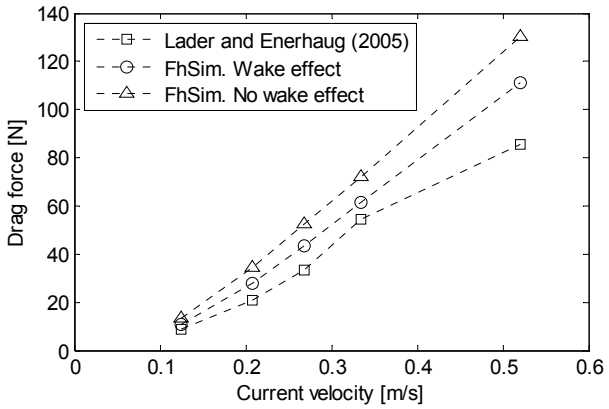

Figure 9: Comparison of drag forces for WC2. Results from simulations with and without wake effect and experiments from [6] are shown.

For the four lowest water velocities in WC2, the model overestimated forces with an average of 23% (Figure 9). Again, the simulation of the highest velocity resulted in larger deviations than the others, with an overestimation of 30%.

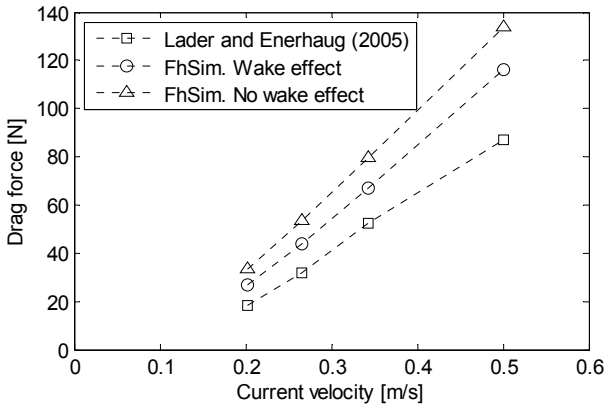

Figure 10: Comparison of drag forces for WC3. Results from simulations with and without wake effect and experiments from [6] are shown.

In the simulations based on the final weight case, the model overestimated the drag forces with an average of 35% (Figure 10). Unlike for the other weight cases, simulations of the highest water velocity did not in percent result in notably larger deviation than lower water velocities.

A comparison between simulation results from cases with and without wake effect reveals that the modeled wake effect reduced the drag forces on the net with 13.2% to 21.6% with an average of approximately 17.1% (Figure 8 to Figure 10). The largest wake effects were in general observed for the two lowest current velocities for all weight configurations. For all weight cases and velocities simulated, the simulations suggested drag forces with a close to linear relation with water velocity. This compares well with the observations of [6] from 0.21 ms^{-1} up to approximately 0.33 m/s. For lower velocities than 0.21 ms^{-1}, [6] indicates a quadratic relation between drag force and velocity.

4. DISCUSSION

Single panel simulations

Results from simulations of the 1 x 1 m panel (Figure 4) show notable wake effects for low angles of attack (α). However, this is also a range of α for which the forces acting on a panel will be low compared to higher α. Consequently, it is likely that the gross effects of the local wake effect on complex structures such as net cages may be less significant than global wake effects acting between panels (for low to moderate deformations). This is also reflected in that while the local wake effect only has an impact for α less than 20°, the global wake effect is defined for α up to 90°. However, for larger deformations of the net cage for which the angle of attack (α) for more segments of the net will be reduced, the importance of local wake effect can increase.

Global wake effect

Comparison between reduced velocity behind a net panel for our wake calculation method and [7] shows similar results. Both methods are based on conservation of momentum and our procedure is comparable to the sum of cylinders method presented in [7, 8] for an angle of attack of 90°. Thus, our results indicate that the basis for our calculations is valid. Our calculations indicate that the angle of attack is important for global wake effect, and suggests a high dependency on angle of attack for angles below 30°. In order to verify the numerical results showing a substantial drop in velocity far behind the panel for an angle of attack of approximately 2.5°, comparison with dedicated experiments is needed. Experiments and calculations in [4] indicate that a sum of cylinders method can be used to evaluate local wake effect. Whether the method is valid for velocities far behind a net panel with low angle of attack is not investigated in the present study.

Comparisons with measurement data for a cylindrical net cage

The general trends in the simulations were similar to the trends seen in the measurements [6], with heavier bottom weights inducing higher drag forces for higher velocities. Heavier weights reduce deformation, yielding a larger projected net area and thus larger drag forces. This suggests that the modeled structure was able to capture how forces acting on cylindrical net cages co-vary with current velocity and weighting. Furthermore, the differences in model output with and without wake effect demonstrated that the implemented wake model provides a consistent reduction in drag forces, implying that the model replicated the most prominent mechanisms behind water velocity reduction downstream of an immersed object.

Model output compared well with measurements for most of the scenarios, especially for WC1 and WC2, implying that the model provided a realistic impression of how wake effects reduce the drag forces on a net cage. The higher deviations between model output and measurements found for higher water velocities may be described by a phenomenon presented in [5], where some of the water passes beneath or around a net cage rather than passing through it, i.e. the velocities around and inside the net cage has a different direction than the incident water current. This effect will become more important for high velocities and high deformations as the projected solidity of the net becomes higher. Since neither the wake representation nor the drag force calculations in the model take this effect into account, the model may overestimate drag forces on structures that experience such effects.

In all simulation scenarios, the model estimates of drag forces were higher than the measured values [6]. This may imply that the implemented wake model in general predicted lower wake effects than the real wake effects occurring within net cages. One cause behind this possible underestimation of wake effects may be that an ideal panel was assumed in the derivation of the local wake formulas, meaning that only the vertical bars were

considered to contribute to local wake effect. For elements that have non-ideal orientation relative to the water current direction, this will lead to too low estimates of the local wake effect since the contribution from horizontal bars not is included.

The magnitudes of local and global wake effects were compared, revealing that the local wake effect had a substantially lower impact on the current velocities than the global wake effect. This suggests that global wake effects may in general have more impact on the drag forces acting on net-cages than local wake effects. For moderately deformed cages, such as those used in this study, this will be the case, as only a few of the net panels comprising the cage would have a sufficiently low α to cause any notable local wake effects. It is thus unlikely that too low estimates of local wake effects alone explain the overestimation of drag forces.

Although the global wake model takes both horizontal and vertical bars into account, it was also based on the assumption that net panels were ideal in terms of mesh axes orientation. For low cage deformations, this will not have a great impact as the meshes in a large proportion of the net will be close to ideally oriented. With higher deformations, the orientation of the meshes will deviate more from ideal orientation. A consequence of this will be that the average distance between mesh bars in the water current direction is smaller, which lead to a more significant wake effect and thus a larger reduction in water velocity. Also, for a non-ideal panel orientation the span of α for which there will be local effects may increase. The model performed better at predicting drag forces for lower water velocities than for higher velocities, which supports this assumption.

Another aspect that can contribute to an underestimation of both local and global wake effect is that the wake model only takes mesh bars into account when calculating reductions in velocity. Knotless Raschel knitted netting have a super knot structure [9], which will introduce extra material in the intersection between twines (see fig. 3 in [6]). This will affect the drag forces and most likely increase the wake effect. As the knot area is accounted for in the drag force computations in FhSim [3], but not in the evaluation of wake effects, this means that the knot area affect drag forces in the model but does not reduce the downstream water velocity. The error in wake estimates will then increase with water velocity, since the knots will be more important for wake effects (and force calculations) as the angle of attack of larger parts of the net decreases due to deformation.

As a net cage deforms due to hydrodynamic forces, the distance between a net section in the downstream wall of the cage and the upstream wall can change. The polynomial approximation of the global wake effect performed for each net element in the numerical model during initialization was based on the initial distance between the centroid of the element and the intersecting plane. Consequently, the polynomial for each element was based on a distance that could be larger than the actual distance between the downstream and upstream panel when the cage is subjected to current. This can in some cases lead to an underestimation of the global wake effect.

The model for computing forces acting on nets in FhSim has previously been validated for angles of attack above 30° using data from net panels tested in a flume tank [3]. However, those panels were built from a net type that differed significantly from the knotless Raschel type, with diamond meshes and large clearly distinguished knots. As such, it is possible that the hydrodynamic load model used in FhSim computes too high drag forces for the type of netting used in [6]. In order to evaluate whether this is a factor in the overestimated drag forces in this study, a comparison between simulations and panel trials similar to those presented in [3], but with the same type of netting used in [6], could be conducted.

Future development of wake model in FhSim

One improvement of the model in FhSim that can result in better estimates of wake effects could be to include the knots in the wake effect formulas. To the authors' knowledge, there exist few sources of information in published literature that could be used to derive a generic wake formulation that takes the intersection between twines and the combined effects of twines and knots into account. However, it could be possible to derive new theory on this subject. Further, the wake computations based on mesh bars could be expanded to include the mesh bar orientation within net elements in addition to the panel angle of attack (α). This is used in the force calculations done in FhSim, where forces are computed separately for the two mesh bar axes by decomposing the incident current velocity vector [3]. When computing the wake effect, such a decomposition of the water velocity will not be valid and care must be taken when developing a method that takes non-ideal panel orientation into account.

CONCLUSION

Drag reduction due to estimated wake effects were consistent for all velocities and weight configurations tested, and calculated drag forces matched measurement data fairly well. The best results were obtained for the lowest current velocities and the weight configurations with the smallest bottom weights.

This study has resulted in a method that was developed from a well-founded theoretical basis and is thus independent of experimental data on net panels. Compared with other approaches based on empirical techniques, the present model may therefore represent a more generic method for predicting wake effects on net structures. Further development of the model and comparison with independent experiments are needed in order to improve the model and thus obtain more accurate estimates of drag forces on flexible net structures.

ACKNOWLEDGMENTS

This work was funded by the Norwegian Research Council project 199574/O70 Numerical simulation of complex systems involving interaction between elements with large and varying stiffness properties.

REFERENCES

[1] Blevins, R. D. 1990. "Flow-Induced Vibration", Van Nostrand Reinhold Co., New York.

[2] Blevins, R. D. 2003. "Applied fluid dynamics handbook." Krieger Publishing Company, Malabar, US.

[3] Enerhaug, B., Føre, M., Endresen, P. C., Madsen, N., and Hansen, K. "Current loads on net panels with rhombic meshes," 31st International Conference on Ocean, Offshore and Arctic Engineering. OMAE2012, Rio de Janeiro, 2012.

[4] Fredheim, A. 2005. "Current Forces on Net Structures". PhD thesis, NTNU, Trondheim, Norway.

[5] Gansel, L., C. McClimans, T. A. Myrhaug, D., 2010, "Average flow inside and around fish cages with and without fouling in a uniform flow", 29th International Conference on Ocean, Offshore and Arctic Engineering, OMAE 2010, Shanghai, China, 2010.

[6] Lader, P., and Enerhaug, B. 2005. "Experimental Investigation of Forces and Geometry of a Net Cage in Uniform Flow". IEEE J. of Ocean Eng., 30 (1).

[7] Løland, G., 1991. "Current forces on and flow through fish farms". PhD thesis, NTNU, Trondheim, Norway.

[8] Løland, G., 1993. "Current forces on, and water flow through and around, floating fish farms". Aquaculture International 1, 72-89.

[9] Moe, H., Olsen, A., Hopperstad, O.S., Jensen, Ø., Fredheim, A., 2007. "Tensile properties for netting materials used in aquaculture net cages". Aquacultural Engineering 37, 252–265.

[10] Priour, D. 1999., "Calculation of net shapes by the finite element method with triangular elements." Commun. Numer. Meth. Engng. 15, 757-765.

[11] Priour, D., 2001. "Introduction of mesh resistance to opening in a triangular element for calculation of nets by the finite element method." Commun. Numer. Meth. Engng. 17, 229-237.

[12] Priour, D., 2003. "Analysis of nets with hexagonal mesh using triangular elements." Int. J. Numer. Meth. Engng. 56, 1721-1733.

[13] Sumer, B., M., Fredse, J., 1997. "Hydrodynamics Around Cylindrical Structures". World Scientific Publishing Co. Pte. Ltd., Singapore.

[14] Tanada, Y., Okajima, A., Watanabe, .Y, 1973. "Stability of a circular cylinder oscillating in uniform flow or in a wake". J. Fluid Mech. (1973), vol. 61. pp 769-784.